Die Angewandte Makromolekulare Chemie **240** *(1996) 123 - 136 (4304)*

Department of Chemistry, The Chinese University of Hong Kong, Shatin, N.T., HONG KONG

VOLUME PHASE TRANSITION OF SPHERICAL MICROGEL PARTICLES

Chi Wu, Shuiqin Zhou, Steve C.F. Au-yeung, Suhong Jiang

Summary: The volume phase transition of poly(*N*-isopropylacrylamide) (PNIPAM) spherical microgel particles was studied by static and dynamic laser light scattering (LLS). The results were compared with the coil-to-globule transition of individual long linear PNIPAM chains. The microgel particles have a higher transition temperature, but a less sharp phase transition, in comparison with that of long linear chains. This difference has been attributed to both the short length and the broad length distribution of the subchains inside the microgels. A combination of static and dynamic LLS results revealed that even in a highly collapsed state the microgel particles retained ~70% of water and the density of the microgel networks increased from 0.021 g/cm^3 to ~0.30 g/cm^3 during the phase transition. The temperature-dependence of the NMR spin-lattice relaxation times T_1 of PNIPAM indicate an association between water and the CH proton on the *N*-isopropyl group. Our results also showed that the transition was strongly influenced by the presence of surfactant. Addition of anionic surfactant, such as sodium dodecyl sulfate (SDS), promotes the swelling of the particles and shifts the transition to a higher temperature, while the addition of a cationic surfactant, such as dodecyl pyridine bromide (DPB), has less effects on the swelling and phase transition, which has been attributed to the electron-rich amide group in PNIPAM. Moreover, a two-step phase transition was observed for the first time in the presence of SDS. The dynamic LLS results demonstrates that SDS is expelled gradually from the microgel in the first-step volume phase transition.

Lecture presented at the "International Symposium on Advanced Network-Polymers, Kansai University" (ISANKU), at Kansai University, Suita, Osaka, Japan, on December 5 - 6, 1995.

 CCC 0003-3146/96/$07.00

INTRODUCTION

In 1968, Dusek *et al.*[1] predicted a possible discontinuous volume phase transition of a polymer gel on the basis of the coil-to-globule transition of a single linear polymer chain. Since then, the volume phase transition of polymer gels has attracted much attention.[2-5] It has been reported that some polymer gels can swell or shrink discontinuously and reversibly in response to many different stimuli, such as temperature,[6] *pH*,[7] electric fields[8] or light,[9] depending on the chemical composition of a given gel/solvent system. The change in volume can be as large as $\sim 10^2$ fold.[10] The large volume change of polymer gels in response to an infinitesimal alternation in environment may also be utilized in controlled-release of biological molecules at specific body conditions, selective absorbents, chemical memories, sensors and artificial muscles.

As one of the many typical examples, poly(N-isopropylacrylamide) (PNIPAM) gels have been extensively studied.[13-25] Their volume can change by hundred folds in water when the temperature varies by ~ 1 °C or less.[11,12] Different models were proposed to explain this thermal volume phase transition.[13-15] Particularly, Grosberg *et al*[16] recently discussed the contribution of topological constraints to this process. However, their theory satisfactorily describes only part of the results in the phase transition range. Since the phase transition of gels is considered as a macroscopic manifestation of the coil-to-globule transition of the subchains inside the gel network, a comparison between spherical PNIPAM microgel particles and individual long PNIPAM linear chains with a similar average size may lead to a better understanding of the swelling and shrinking behaviour of the PNIPAM gel at molecular level.

Most in the past have dealt with the swelling and shrinking of bulk PNIPAM gels by using various methods, such as microscopy,[17] dilatometry,[18] differential scanning calorimetry,[19] friction measurement,[20] small angle neutron scattering[21] and NMR.[22] However, relatively few studies of PNIPAM microgels have been reported.[23-26] Tanaka *et al*[27-30] demonstrated that for a spherical gel the time required for swelling or shrinking is proportional to the square of its radius, whereas for microgel particles with a smaller radius, a much faster response to its environmental change occurs. In addition, the results obtained from some studies of spherical PNIPAM microgels showed that the volume phase transition is continuous, rather than the discontinuous transition observed for bulk PNIPAM gels. This difference has been attributed to the irregular particle surface formed during the phase transition.

Another important aspect of the volume phase transition of PNIPAM or hydrophobically modified PNIPAM gels is that surfactant can promotes both inter- and intra-molecular solubility

so that the transition temperature increases with increasing surfactant concentration. An association of the surfactant hydrophobic tails with the hydrophobic side groups or backbone of PNIPAM has been suggested. Recently, Khokhlov *et al.*[31] predicted that the interaction of a polyelectrolyte gel with an oppositely charged surfactant presents three effects: (i) At low surfactant concentration, the surfactant cannot form micelles inside the network. The gel behaves as though they are in the solution of low molecular-weight salts, shrinking slightly. (ii) At higher surfactant concentration, surfactant molecules inside the gel exceed the critical micelle concentration (CMC) so that micelles are formed inside the gels. The attraction between the micelles and gel network leads to the collapse of the gel. (iii) At still higher surfactant concentration, no additional micelles can be formed inside the gel network and the network dimension should be similar to that of a corresponding neutral gel network.

EXPERIMENTAL

Materials. *N*-isopropylacrylamide (NIPAM) (courtesy of Kohjin, Ltd., Japan) was recrystallized three times in a benzene/n-hexane mixture. *N,N'*-methylenebis(acrylamide) (BIS) as crosslinker was recrystallized from methanol. Potassium persulfate (KPS) (from Aldrich, analytical grade and was used as an initiator), sodium dodecyl sulfate (SDS) (BDH, 99%, anionic surfactant) and dodecyl pyridine bromide (DPB) (Beijing University, China, 99%, cationic surfactant) were used without further purification.

Sample preparations. 240 mL dust-free deionized water, 3.84 g NIPAM, 0.0730 g BIS, and 0.0629 g SDS were added to a 500-mL reactor fitted with a glass stirring rod, a Teflon paddle, a condenser, and a nitrogen bubbling tube. The solution was heated to 70 °C and stirred at 200 rpm for 40 min with a nitrogen purge to remove oxygen followed by addition of 0.1536 g KPS in 25 mL dust-free deionized water to start the polymerization. The reaction was carried out for ~4.5 hr. The microgel particles were purified and diluted to $\sim 10^{-6}$ g/mL for LLS measurements. Hereafter, we will refer this original PNIPAM microgel particles as surfactant free, or $C_{SDS} \sim 0.0$ g/mL, in contrast to those solutions wherein surfactant SDS or DPB were added. The resistivity of the deionized water used in this study was 18.3 MΩ·cm. The narrowly distributed linear long PNIPAM linear chains ($M_w = 1.08 \times 10^7$ g/mol and $M_w/M_n < 1.06$) was prepared by a combination of fractionation and filtration of a broadly distributed PNIPAM sample which was made in a conventional free-radical polymerization. The water-free solvent and filtration are two key factors for the success of the preparation. The detail of this sample preparation has been reported earlier.[32]

Nuclear magnetic resonance (NMR). The ^1H and ^{13}C NMR spin-lattice relaxation times T_1 measurements were carried out using a Bruker ARX-500 superconducting Fourier transform NMR spectrometer operating at 500.13 (^1H) and 125.76 (^{13}C) MHz, respectively.

Laser light scattering (LLS). The excess absolute scattered light intensities and intensity-intensity time correlation functions of spherical PNIPAM microgel particles and individual linear PNIPAM chains were measured over a wide scattering angle range of 6-150° with a modified commercial LLS spectrometer (ALV/SP-150 equipped with an ALV-5000 multi-tau digital time correlator). A solid state laser (ADLAS DPY425II, output power is ~400 mw at λ = 532 nm) was used as the light source. The incident beam was vertically polarized with respect to the scattering plane. The detail of LLS instrumentation and theory can be found elsewhere.[33,34] All light-scattering solutions were clarified by a 0.5-μm filter to remove dust.

In Static LLS, for a dilute solution and at a relatively low scattering angle θ, the angular dependence of the excess absolute time-averaged scattered intensity, known as the excess Rayleigh ratio $R_{vv}(q)$, is related to the weight average molecular weight M_w, the second virial coefficient A_2, and the root-mean square z-average radius of the polymer chain $\langle R_g^2 \rangle_z^{1/2}$ (or written as R_g) according to[35]

$$\frac{KC}{R_{VV}(q)} = \frac{1}{M_w}\left(1 + \frac{1}{3}R_g^2 q^2\right) + 2A_2 C \qquad (1)$$

where $K = 4\pi(dn/dC)^2 n^2/(N_A \lambda_o^4)$ and $q = (4\pi n/\lambda_o)sin(\theta/2)$ with N_A, dn/dC, n and λ_o being the Avogadro number, the specific refractive index increment, the solvent refractive index, and the wavelength of light in vacuo, respectively. After measuring $R_{vv}(q)$ at a series of C and θ, we are able to determine M_w, R_g, and A_2 from a Zimm plot which incorporate angular and concentration extrapolation on a single grid.

In dynamic LLS, the measured intensity-intensity time correlation function $G^{(2)}(t,q)$ in the self-beating mode is related to the first-order electric field time correlation function $|g^{(1)}(t,q)|$ as[33,34]

$$G^{(2)}(t,q) = A[1 + \beta|g^{(1)}(t,q)|^2] \qquad (2)$$

where A is a measured baseline; β, a parameter depending on the coherence of the detection; and t, the delay time. For a polydisperse sample, $|g^{(1)}(t,q)|$ is related to the normalized characteristic

line-width distribution G(Γ) by

$$g^{(1)}(t,q) = \int_0^\infty G(\Gamma)e^{-\Gamma t}d\Gamma \qquad (3)$$

Using a Laplace inversion program CONTIN[36] equipped with the correlator, we were able to calculate G(Γ) from $G^{(2)}(t,q)$ on the basis of eqs 2 and 3. In general, Γ is a function of both C and q.[37] For a diffusive relaxation, $D \equiv \Gamma/q^2$ if the solution is dilute and $\langle R_g \rangle q << 1$, where D is the translational diffusion coefficient. Furthermore, D can be converted into the hydrodynamic radius of R_h using the Stokes-Einstein equation $R_h = k_B T/(6\pi\eta D)$, where k_B, T and η are the Boltzmann constant, the absolute temperature and the solvent viscosity, respectively.

RESULTS AND DISCUSSION

Figure 1 shows a comparison of the temperature dependence of the reduced average hydrodynamic radius $\langle R_h \rangle / \langle R_h \rangle^*$, where $\langle R_h \rangle^*$ is the average hydrodynamic radius at the collapsed state. At 20 °C, there is little swelling of the microgel particles in comparison with that of the linear chains because the crosslinking inside the gel hinders the swelling. For both the spherical particles and the linear chains, the change of $\langle R_h \rangle$ is continuous. It is worth noting that the decrease of $\langle R_h \rangle$ for the linear chains is sharper than that for the microgel; and the transition temperature of the particles is higher than that of the linear chains. This is explained as follows.

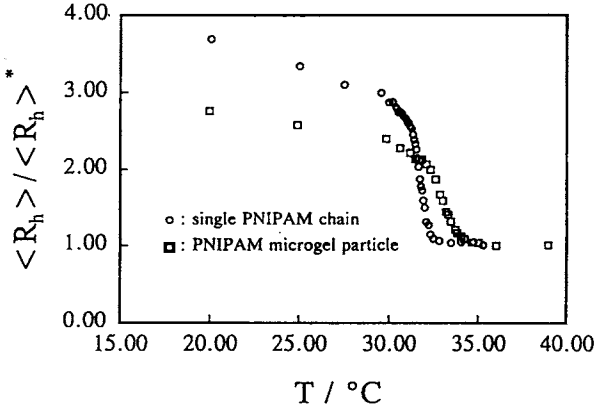

Fig. 1. Temperature dependence of the reduced average hydrodynamic radius $\langle R_h \rangle / \langle R_h \rangle^*$, where $\langle R_h \rangle^*$ is the average hydrodynamic radius at the collapsing limit.

For a given linear polymer chain with a lower critical solution temperature (LCST), it is known that the transition temperature increases with increasing molecular weight.[38] Therefore, for a polydisperse sample, polymer chains with different lengths will undergo the transition at different temperatures and the phase transition of the whole sample becomes less sharp. In a similar way, the phase transition temperature of a polymer gel network is directly related to the molecular weight (M_C) of the subchain between two neighboring crosslinking points. The gel with a higher M_C will undergo the phase transition at a lower temperature.[39] In this study, the average subchain length (~ 20 nm) inside the microgel particles is ~10^2 times shorter than the average length of the linear PNIPAM chains and the subchain length distribution is much broader. This is why the microgel particles have a higher transition temperature and a less sharper transition. However, it should be noted that the real picture is actually more complicated than what we have just described, but the essence of the physics remains. A gel could be visualized as a polymer network made of a set of subnetworks, each has a different M_C. The subnetworks with different subchain lengths will undergo the transition at different temperature, namely the phase transition covers a range of temperatures. Therefore, the phase transition for a polymer gel is intrinsically continuous.

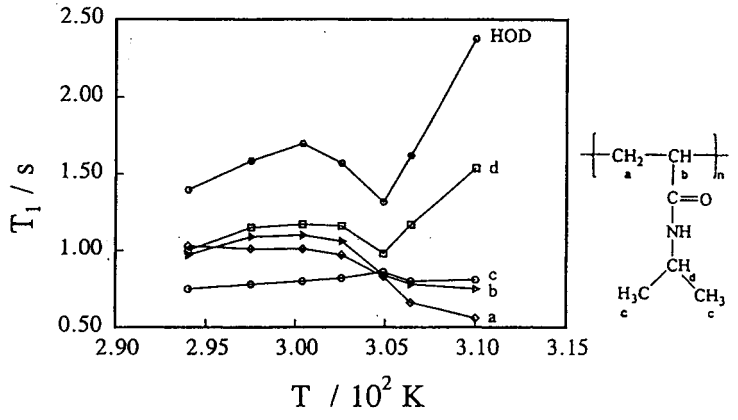

Fig. 2. Temperature-dependence of the spin-lattice relaxation time T_1 for different protons.

Figure 2 shows the temperature-dependence of T_1 of the different protons in PNIPAM. It is interesting to note that during the phase transition T_1 decreases with increasing temperature for all the protons, except for the CH proton (d) in the *N*-isopropyl group. The T_1 of the CH proton behaves similarly to that of HOD over the entire temperature range. This result suggests that HOD is associated with the CH proton in the *N*-isopropyl group because T_1 depends on the energetic characterized by the relaxation pathway involving related groups.

Figure 3 shows plots of the refractive increment (Δn) versus concentration (C) for the spherical microgel particles at two temperatures respectively below and above the volume phase transition temperature (~33 °C). The Δn values were determined by using a novel differential refractometer which was recently developed and incorporated as part of our light scattering spectrometer.[40] The laser light was split into one strong (~1%) and one weak (~99%) beams which were used as the light source for LLS and refraction, respectively. In this way, we were able to measure the refractive increases Δn and the scattered light intensity under identical conditions, so that the wavelength correction was eliminated. The dn/dC values calculated from the slope of the lines are 0.181 and 0.201 mL/g for the microgel particles in water at 30.01 °C and 35.01 °C, respectively. The higher dn/dC value at 35.01 °C reflects the higher density of collapsed microgel particles.

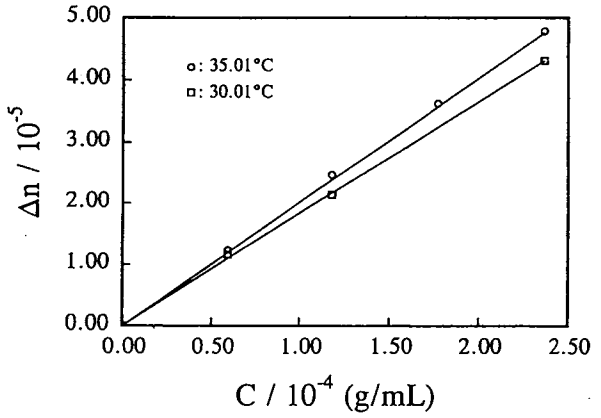

Fig. 3. Plots of the refractive increment (Δn) versus concentration (C) for the PNIPAM microgel particles at two temperatures below and above the phase transition temperature (~33 °C)

Table I summarizes the static and dynamic LLS results for the microgel particles at two temperatures below and above the phase transition temperature (~33 °C). A nearly constant value of M_w shows that the microgel particles are stable in the collapsed state, otherwise an increase in M_w would be observed, i.e., aggregation. As expected, A_2 changes from positive to negative values because water is a good solvent at 25.01 °C for the microgel particles but becomes a poor solvent at 35.01 °C. This is why the microgel particles collapsed into a 10-time smaller volume. The ratio of R_g/R_h is very close to the theoretical value $(3/5)^{1/2}$ predicted for a uniform sphere, which indicates that the microgels studied are uniform spherical particles either in the swollen or collapsed state. There is no draining for water entrapped inside the microgel particles, otherwise

we would observe a larger value of R_g/R_h. The chain density ρ of the PNIPAM microgel network is calculated by a combination of the static and dynamic LLS results, namely from M_w and R_h according to: $M_w = (3\pi/4)R_h^3\rho$.

Table I. LLS results for the PNIPAM microgel particles in water at two different temperatures

T / °C	dn/dC / mL·g^{-1}	M_w / g/mol	A_2 / mol·mL/g^2	R_g / nm	R_h / nm	R_g/R_h	ρ / g/cm^3
30.01	0.181	2.19×10^8	3.02×10^{-6}	124	160	0.78	0.02
35.01	0.201	2.25×10^8	-2.25×10^{-5}	57	70	0.81	0.30

Table I shows that ρ is ~0.30 g/cm^3 in a fully collapsed state, which is in agreement with that of bulk gels studied by small angle neutron scattering.[21] Grosberg *et al.*[16] explained this low chain density in terms of the concept of the crumpled globule state.[16] In comparison with the chain density ($\rho \sim 0.02$ g/cm^3) of the microgel particles in the swollen state, we know that ~94% of water entrapped inside the microgel particles is excluded from the microgel particles during the volume phase transition after considering both the changes in R_h and ρ.

Figure 4 shows the time-dependence of $\langle R_h \rangle$ for the microgel particles after a rapid temperature change. The time t is the standing time after the solution was quenched from 35.0 °C to 30.0 °C, or inversely jumped from 30 °C to 35 °C. In order to speed up the temperature equilibrium, a very special thin-wall (~ 0.4 mm) LLS cell was used. Both the speed of the swelling and collapsing processes remain too fast to be accurately followed with our present LLS instrumentation. According to Tanaka *et al*[27-30], the transition time for the microgel particles studied should be in the range of ~10^{-3} s. Therefore, the size change shown in Fig. 4. actually reflects the temperature change. In comparison with our previous study,[32] the coil-to-globule transition of individual long linear PNIPAM chains is much slower. This difference in the transition speed arises from the fact that on average the subchain between two neighbouring crosslinkers inside the microgel particles is ~ 10^2 times shorter than the long linear PNIPAM chains. Moreover, the swelling or shrinking speed of a gel in response to an excess osmotic pressure is controlled by the collective diffusion of solvent into the gel.

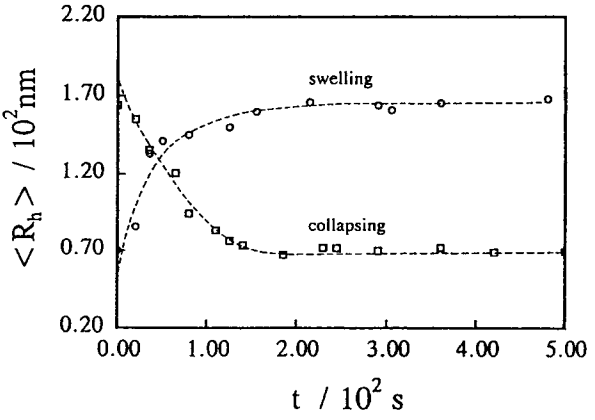

Fig. 4. Collapsing and swelling of the microgel particles after a rapid temperature change.

Figure 5 shows the influence of the surfactant SDS on the phase transition of the microgel particles. It clearly reveals that the particles were swollen by SDS. When C_{SDS} = 9.5 mM, the swollen particles were so stable that the transition temperature became too higher to be measured. Besides the increase of the transition temperature, the phase transition became a two-step process after addition of SDS. This two-step transition became more obvious as C_{SDS} increases. It should be noted that the second step appeared when $\langle R_h \rangle$ ~180 nm and corresponds to the size of the surfactant-free microgel particles in the swollen state. To our knowledge, a two-step volume phase transition of this type has not been observed before.

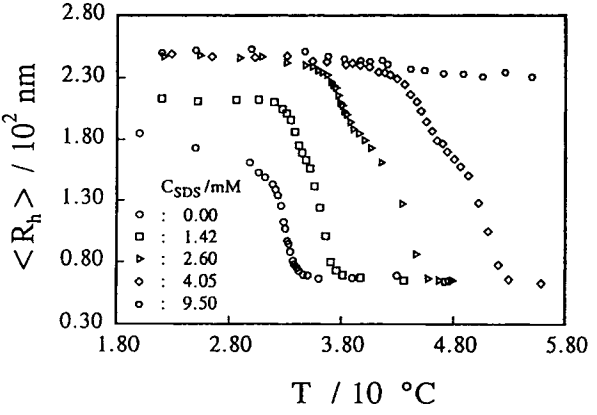

Fig. 5. Influence of surfactant SDS on the phase transition of the PNIPAM microgel particles.

Figure 6 shows how the translational diffusion coefficient distribution of the microgel particles changes with temperature during the phase transition. As temperature increases, G(D) shifts to higher D, i.e., smaller R_h, because of the collapse of the particles. Initially, there existed only one narrowly distributed peak. When temperature increases above 45 °C, another small peak appears (it is enlarged in the logarithmic scale) at much higher D, representing some smaller species. The surprising appearance of this second peak may be related to the SDS molecules which were driven out during the volume phase transition.

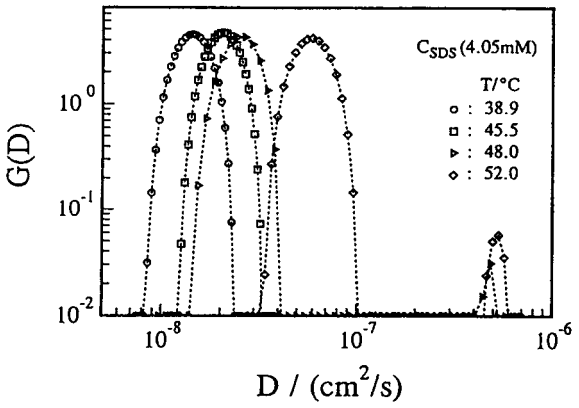

Fig. 6. Temperature-dependence of the translational diffusion coefficient distribution G(D) for the PNIPAM microgel particles with 4.05 mM of added SDS molecules.

It is generally recognized that SDS can 'bind" the hydrophobic portion of PNIPAM, so that the PNIPAM chain behaves like a polyelectrolyte chain. The repulsion between the anionic heads of SDS swells the PNIPAM chain or gel network when temperature is below the phase transition temperature.[41] However, we could not exclude the possible formation of the SDS micelles inside the microgel network because the SDS concentration inside the microgel network could be higher than its critical micelle concentration (CMC), even though the overall SDS concentration is lower than the CMC. During the first-step phase transition, the SDS micelles might be "crashed" into individual SDS molecules by the shrinking microgel network. The flat transition between the two steps might be attributed to the exclusion of individual SDS molecules from the particles, so that we observed the second small peak in Fig. 6. After the exclusion of SDS, the microgel particle should be similar to the SDS-free microgel particles. This is why at the end of the first step they have a similar size. Further increase of temperature will induce an additional collapse of the particles, i.e., the second step, which is similar to the collapse of the SDS-free particles, but at a much higher temperature. A comparison of Figs. 5 and 6 shows that the second peak did appear

at the end of the first step, which is consistence with the above discussion.

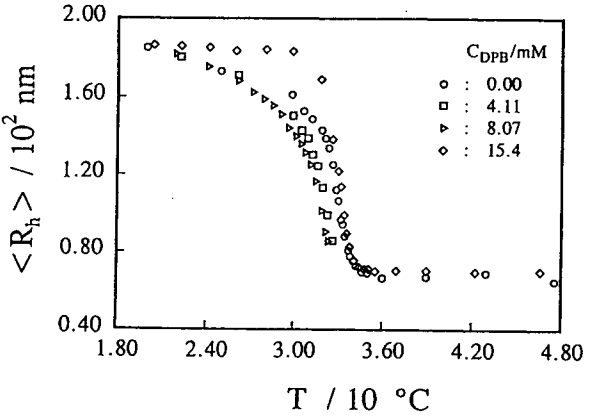

Fig. 7. Influence of surfactant DPB on the phase transition of the PNIPAM microgel particles.

Figure 7 shows that when C_{DPB} is lower than the CMC (~12 mM) of DPB in water, the transition temperature is slightly lower than that of the surfactant-free particles. The microgel particles in the collapsed state were unstable, so that $<R_h>$ did not reach the size of the completely collapsed particles. When C_{DPB} is higher than the CMC, the phase transition temperature is slightly higher and the volume phase transition is sharper than that of the surfactant-free particles. Moreover, the microgel particles are thermodynamically stable over the entire temperature range studied. A comparison of Figs. 5 and 7 shows that SDS and DPB have completely different effects on the behavior of the microgel particles. Therefore, the generally recognized "binding" of SDS to the hydrophobic portion of PNIPAM might not be true because SDS and DPB have an identical hydrophobic tail. we offer a possible explanation for this complete difference as follows.

The interaction between the anionic head of SDS and the anionic residual group (generated from the initiator) or the amide group (with one pair of electrons) in the PNIPAM chain should be repulsive. SDS molecules have a chance to form micelles inside the microgel network and the repulsion leads to the swelling of the particles and the hindering of the phase transition. Meewes *et al.*[42] showed that for PNIPAM chain without the anionic residual group swelling took place in the presence of SDS. This result suggests to us that the main contribution comes from the electron-rich amide group. On the other hand, the cationic head of DPB has a tendency to be "attracted" to the anionic residual group or the amide group to form an ion pair or a tetra-amine complex. In this way, it would be difficult for DPB molecules to move together to form micelles inside the microgel network. Moreover, the "attraction" of the cationic head to the anionic or the

amide group partially cancel the hydrophilic nature of PNIPAM. This explains why the phase transition temperature is lower and the microgel particles were unstable at higher temperatures When C_{DPB} is higher than the CMC, the DPB micelles should form both inside and outside of the microgel networks if the microgel is in the swollen state. The repulsion between the DPB micelles can lead to a further swelling of the particles, as shown in Fig. 7. This repulsion between the DPB micelles inside the microgel network can retard the collapse of the particle up to a point at which the dedicate balance between the hydrophobic and hydrophilic interactions start to break. From that point, further increase in temperature will lead to the collapse of the particles and the exclusion of DPB from the microgel network. This explains the sharp transition shown in Fig. 7. It should be stated that in the collapsed state the particle size is independent of the amount and type of surfactant added, which indirectly shows that in the collapsed state there is no surfactant, or more precisely, an insignificant amount of surfactant, inside the particles.

In summary, the volume phase transition of the PNIPAM microgel particles is continuous over a range of temperatures, corresponding to a broad subchain length distribution inside the microgel network. A combination of the static and dynamic laser light scattering results showed that there is no draining for water entrapped inside the microgel particles even in the swollen state. During the volume phase transition, ~94% of water originally entrapped inside the swollen microgel network is expelled. On the other hand, in its fully collapsed state, the microgel particle still entraps ~70% of water in its occupied space. Anionic and cationic surfactant molecules interact differently with the microgel particles, namely a very small amount of anionic surfactant SDS can swell the particles and shift the phase transition to a higher temperature, while the addition of cationic DPB has much less effect on either the swelling or the phase transition temperature. This has been attributed to the presence of both the electron-rich amide group and the residual anionic groups generated from the initiator on the PNIPAM chain.

ACKNOWLEDGEMENT. The financial support of the RGC (the Research Grants Council of Hong Kong Government) Earmarked Grant 1994/95 (CUHK 299/94P, 221600260) is gratefully acknowledged. Chi Wu would like to thank Professor Akira Matsumoto and the Organizing Committee of the International Symposium on Advanced Network-Polymers, Kansai University" (ISANKU) for their kind invitation. Chi Wu is also grateful to the financial support of Kansai University which made the presentation of this work at ISANKU possible.

REFERENCES AND NOTES

1 K. Dusek, D. Patterson, J.Polym.Sci., Phys.Ed. 6 (1968) 1209

2 J. Hasa, M. Ilavsky, K. Dusek, J.Polym.Sci., Polym.Phys.Ed. 13 (1975) 253

3 T. Tanaka, ACS Symp.Ser. 480 (1991) 1 and references therein

4 M. Shibayama, T. Tanaka, Advances in Polym. Sci. 109 (1993)1 and references therein

5 Y. Osada, S.B. Ross-Murphy, Sci.Am. 264 (1993) 42

6 M. Ilavsky, Macromolecules 15 (1982) 782

7 T. Tanaka, D. Fillmore, S.T. Sun, I. Nishio, G. Suislow, A. shah, Phys.Rev.Lett. 45 (1980) 1636

8 T. Tanaka, I. Nishio, S.T. Sun, S.U. Nishio, Science 218 (1982) 467

9 A. Suzuki, T. Tanaka, Nature 346 (1990) 345

10 B. Erman, P.J. Flory, Macromolecules 19 (1986) 2342

11 Y. Hirokawa, T.Tanaka, E.S. Matsuo, J.Chem.Phys. 81 (1984) 6379

12 R.F.S. Freitas, E.L. Cussler, Sep.Sci.Technol.22 (1987) 911

13 S. Hirotsu, Y. Hirokawa, T. Tanaka, J.Chem.Phys. 87 (1987) 1392

14 K. Otake, H. Inomata, M. Konno, S. Saito, J.Chem.Phys. 91 (1991) 1345

15 M. Marchetti, S. Prager, E.L. Cussler, Macromolecules 23 (1990) 1760,3445

16 A.Y. Grosberg, S.K. Nechaev, Macromolecules 24 (1991) 2789

17 K. Otake, H. Inomata, M. Konno, S. Saito, Macromolecules 23 (1990) 283

18 Y. Hirokawa, E. Sato, S. Hirotsu, T. Tanaka, Polym.mater.Sci. Eng. 52 (1985) 520

19 Y. Li, T. Tanaka, J.Chem.Phys. 90 (1989) 5161

20 M. Tokita, T. Tanaka, Science 253 (1991) 1121

21 M. Shibayama, T. Tanaka, J.Chem.Phys. 97 (1992) 6829

22 M.V. Badiger, P.R. Rajamohanan, M. Kulkarni, S. Ganapathy, Macromolecules 24 (1991) 106

[23] T. Tanaka, E. Sato, Y. Hirokawa, S. Hirotsu, J. Peetermans, Phys.Rev.Lett. 55 (1985) 2455

[24] E. Sato, T. Tanaka, J.Chem.Phys.89 (1988) 1695

[25] Y. Hirose, T. Amiya, Y. Hirokawa, T. Tanaka,Macromolecules 20 (1987) 1342

[26] UK Pat. GB2262117A (1993), M.J. Snowden, B. Vincent, J.C. Morgan

[27] R.H. Pelton, P. Chibante, Colloids Surf. 20 (1986) 247

[28] W. Mcphee, K.C. Tam, R.H. Pelton, J.Colloid and Interface Sci. 156 (1993) 24

[29] M. Murray, F. Rana, I. Haq, J. Cook, B.Z. Chowdhry, M.J. Snowden, J. Chem. Soc., Chem. Commu. 18 (1994) 1803

[30] B.E. Rodriguez, M.S. Wolfe, Macromolecules 27 (1994) 6642

[31] A.R. Khokhlov, E.Y. Kramarenko, E.E. Makhaeva, Makromol. Chem., Theory Simul. 1 (1992) 105

[32] C. Wu, S.Q. Zhou, Macromolecules 28 (1995) 5388

[33] B. Chu, Laser Light Scattering, 2nd Ed., Academic Press, New York 1974

[34] R. Pecora, B.J. Berne, Dynamic light Scattering, Plenum Press, New York 1976

[35] B.H. Zimm, J.Chem.Phys. 16 (1948) 1099

[36] S.W. Provencher, Biophys.J. 16 (1976) 29; J.Chem.Phys 64 (1976) 2772

[37] W.H. Stockmayer, M. Schmidt, Macromolecules 17 (1984) 509

[38] P.J. Flory, Principles of Polymer Chemistry, Cornell University Press, New York 1953

[39] M. Shibayama, M. Morimoto, Nomura, S. Macromolecules 27 (1994) 5060

[40] C. Wu, K. Chan, K.Q. Xia, Macromolecules 28 (1995) 1032

[41] K.C. Tam, S. Ragaram, R.H. Pelton, Langmuir 10 (1994) 418.

[42] M. Meewes, J. Ricka, M. de Silva, R. Nyffenegger, Th. Binkert, Macromolecules 24 (1991) 5811